JOURNAL OF MATERIALS SCIENCE 18 (1983) 3023–3030

Mixed electrical conduction in sintered b c c $6Bi_2O_3 \cdot SiO_2$

MASARU MIYAYAMA, YOSHIHIRO SUENAGA, HIROAKI YANAGIDA
Department of Industrial Chemistry, Faculty of Engineering, University of Tokyo, 7-3-1 Hongo, Bunkyo-ku, Tokyo 113, Japan

The electrical behaviour of bcc $6Bi_2O_3 \cdot SiO_2$ sintered specimens was investigated by measuring electrical conductivity, ionic transference number, Seebeck coefficient and cationic composition. The total conductivity, σ_t, in the P_{O_2} range from 10^5 to 10^{-7} Pa showed mixed conduction where electron conductivity was predominant below 10^{-1} Pa and where σ_t could be expressed by the equation

$$\sigma_t = \sigma_i + \sigma_p^0 \cdot (P_{O_2}/10^5\ \text{Pa})^{1/4} + \sigma_n^0 \cdot (P_{O_2}/10^5\ \text{Pa})^{-1/4}$$

where σ_i, σ_p^0 and σ_n^0 represent the oxygen ionic, hole and electron conductivities, respectively, at a P_{O_2} of 10^5 Pa. The silicon concentration in the specimen was slightly less than the theoretical value. The cation atomic ratio, Si/Bi (theoretically 1/12), was estimated as 0.93 ~ 0.95/12. Schottky-type defects of silicon and oxygen vacancies were proposed to explain a much higher oxygen ionic conductivity in the sintered specimens than that reported for single crystals.

1. Introduction

Among the four polymorphs of pure Bi_2O_3, body-centred cubic (γ) form is metastable but can be stabilized by the addition of small amounts of dopant oxides to form the sillenite group of compounds $6Bi_2O_3 \cdot MO_x$ [1, 2]. The structure of the sillenite compounds has been determined: the M cations are tetrahedrally coordinated and occupy the body-centred sites and the cube corners, linked by hepta-coordinated bismuth atoms. This lattice only achieves the perfect structure where the M cation is tetravalent giving the general formula $6Bi_2O_3 \cdot MO_2$ [3, 4]. The bcc $6Bi_2O_3 \cdot SiO_2$, a typical sillenite compound, is stable up to 900° C (melting point) [2] and is known to show strong piezoelectric and electro-optic effects and high photoconductivity [5–7]. Hence it is expected to be well suited for photographic and optical wave guide devices.

The electrical conduction of bcc $6Bi_2O_3 \cdot SiO_2$ single crystal is reported to be p-type electronic at room temperature and to have very little contribution from oxygen ionic transport at high temperatures [5, 8]. However, the conduction mechanism for sintered or nonstoichiometric bcc $6Bi_2O_3 \cdot SiO_2$ is not clear. It is of interest in view of the ionic conduction which is known to be significant for cubic Bi_2O_3 solid solutions [9, 10].

In the present study, the electrical conduction of sintered bcc $6Bi_2O_3 \cdot SiO_2$ was investigated by measuring electrical conductivity as a function of temperature and oxygen partial pressure (P_{O_2}), and by measuring the ionic transference number, Seebeck coefficient and cationic composition.

2. Experimental details

The raw materials were Bi_2O_3 (99.99% pure) and SiO_2 (99.99% pure). The powders were mixed with a molar ratio of 6:1, melted at 1000° C in a platinum crucible and quenched to room temperature in air. The quenched sample was subsequently annealed at 700° C for 2 h and furnace-cooled [11]. Powder X-ray diffraction analysis showed the single phase to be the cubic δ form for the quenched sample and the bcc γ form for the annealed sample, respectively. The lattice parameter of the bcc γ form was 1.010 nm, which was in good agreement with the reported 1.0106 nm [8].

0022–2461/83 $03.00 + .12

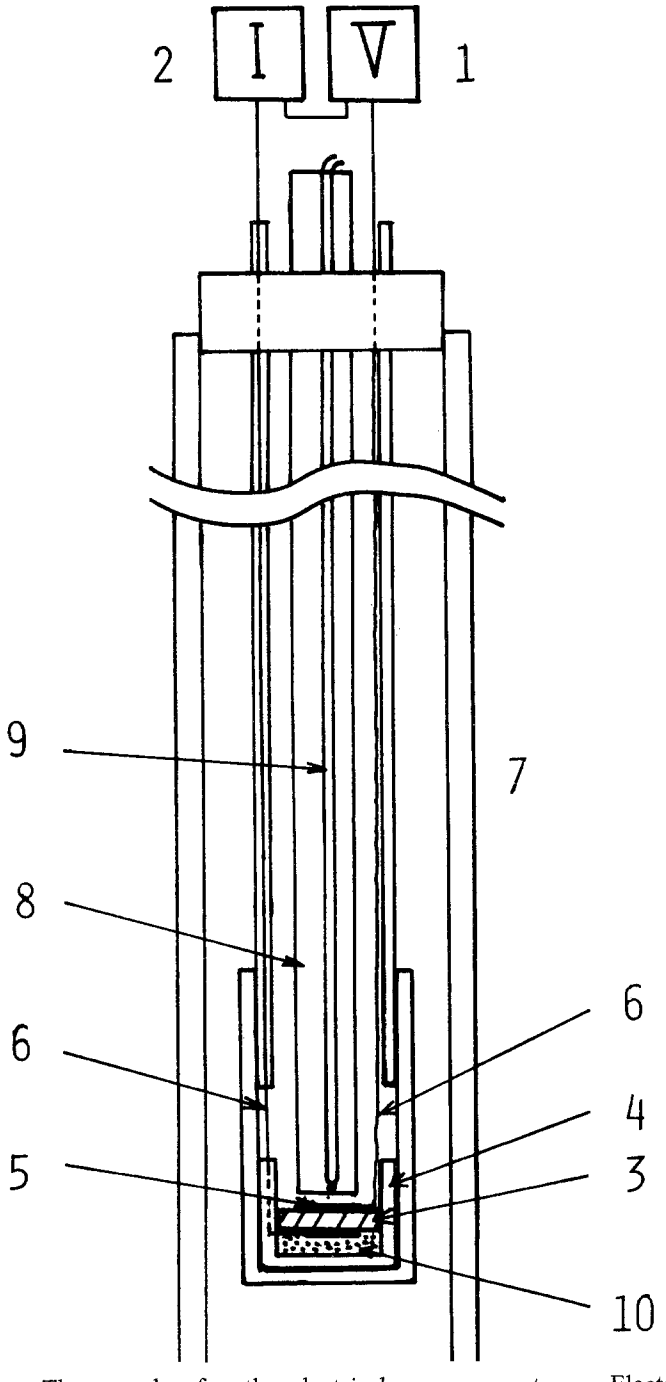

Figure 1 Construction of polarization cell. 1. D.c. constant power supply. 2. Ammeter. 3. Electrolyte. 4. Quartz glass holder. 5. Gold sputtered electrode. 6. Platinum wire. 7. Alumina tube (50 nm diameter). 8. Alumina rod. 9. Thermocouple (a.c.). 10. Blocking electrode (In metal).

The samples for the electrical measurements were made by pressing the b c c form powder into pellets or rods under a pressure of 52 MPa and sintering in air at 820° C for 2 h. The apparent density of the sintered specimens was about 86 to 88% of the theoretical value. Preparing sintered specimens by a conventional method without the melting stage gave a minor second phase in the bcc form. Polymorphic transformations were examined by differential thermal analysis.

Electrical conductivity measurements were performed by a four-probe d.c. method using baked platinum paste as electrodes at constant temperatures. Ionic transference numbers were determined by a d.c. polarization method. A sputtered gold cathode was covered with indium metal as a blocking electrode, and a gold anode was exposed to air, as shown in Fig. 1. The following equation was used to calculate the transference number t_i;

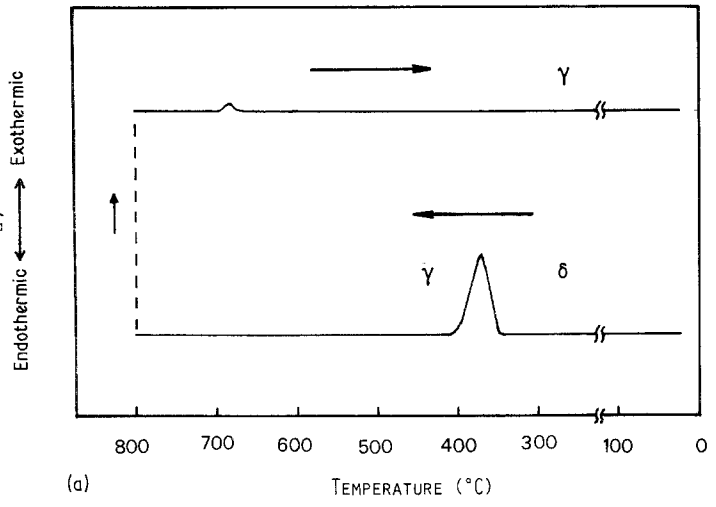

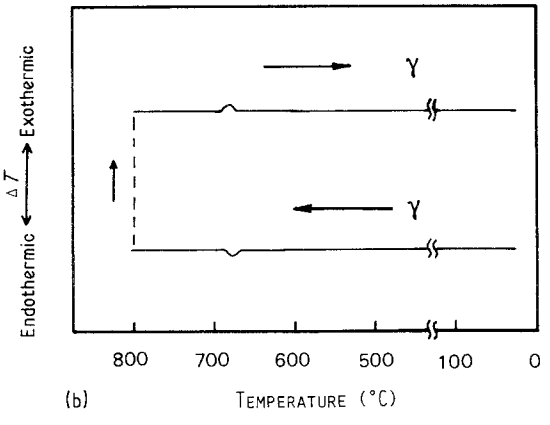

Figure 2 DTA curves for quenched (a) and annealed (b) $6Bi_2O_3 \cdot SiO_2$.

$$t_i = 1 - \sigma(\infty)/\sigma(0) \quad (1)$$

where $\sigma(0)$ is the a.c. conductivity at a frequency of 10 kHz and $\sigma(\infty)$ is the d.c. conductivity after polarization. The Seebeck coefficient was measured at 700° C with two Pt–Pt13%Rh thermocouples attached to two ends of the specimen. The temperature difference (about 6 K) was controlled using a temperature gradient in the electric furnace. For the P_{O_2} dependences of the conductivity and the Seebeck coefficient, $Ar-O_2$ mixed gas was passed as a carrier gas and stabilized zirconia cells were used for reducing and monitoring the P_{O_2}. The experimental set-up is shown elsewhere [12]. Cationic composition in the compound was determined by atomic absorption spectroscopy of nitric sample solutions and by spectrophotometry using colouration of molybdosilicic acid with silicon [13].

3. Results and discussion

Fig. 2 shows the DTA curves for the quenched and annealed $6Bi_2O_3 \cdot SiO_2$. Powder X-ray diffraction analysis showed that a large exothermic peak at about 450° C on heating the quenched sample is attributed to a transformation of the cubic δ form to the bcc γ form. After cooling from 800° C to room temperature both samples were single phase of bcc γ form. It was not possible to determine by X-ray analysis the kind of reactions that occurred at the small exothermic and endothermic peaks at 670 to 680° C in both samples. However, it is assumed from conductivity and composition measurements that a small amount of the δ form exists above the temperature of those small peaks.

Electrical conductivity of bcc $6Bi_2O_3 \cdot SiO_2$ against the reciprocal of the absolute temperature is shown in Fig. 3. Data for a single crystal [8] are also shown in Fig. 3. The conductivity of the sintered specimen is higher than that of the single crystal and shows an abrupt increase above 700° C. A similar phenomenon was presented for the bcc $6Bi_2O_3 \cdot PbO$ compound [8]. Probably this abrupt increase of conductivity would be due to the highly conductive cubic δ form partially transformed from the bcc γ form, as in the case of $6Bi_2O_3 \cdot PbO$.

The dependences of conductivity on oxygen partial pressure (P_{O_2}) for bcc $6Bi_2O_3 \cdot SiO_2$ at several temperatures are shown in Fig. 4. The P_{O_2} dependence showed a behaviour of mixed conduction where the n-type P_{O_2} dependence in the low P_{O_2} region was $P_{O_2}^{1/4}$. The contributions of p-type and n-type electronic conduction increased with increasing temperature.

Ionic transference numbers measured by the polarization method are shown in Fig. 5. In the present study, the applied voltage was controlled to change the oxygen activity at the blocking elec-

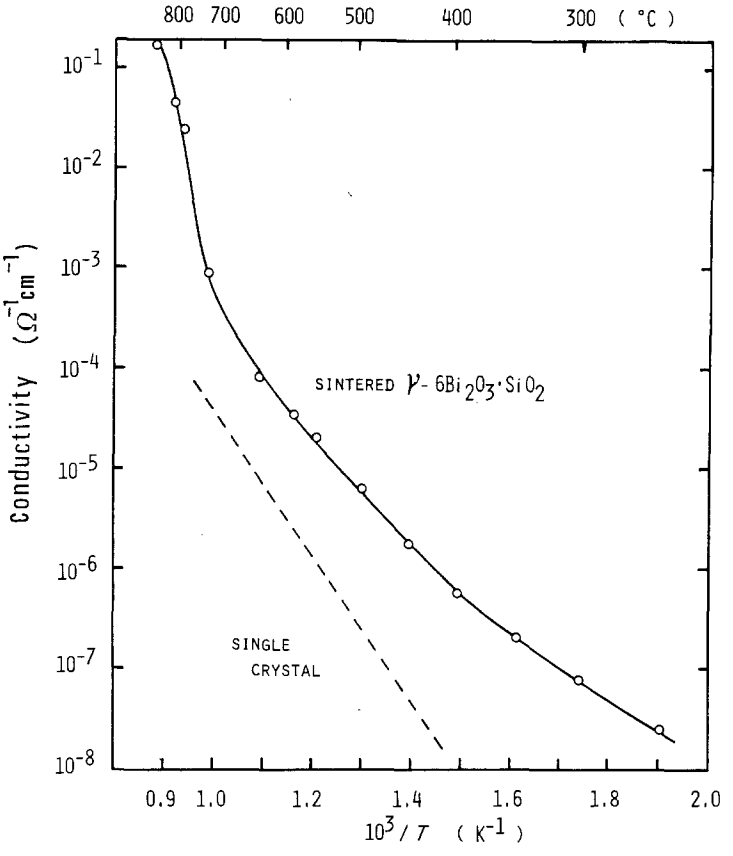

Figure 3 Electrical conductivity–temperature characteristics in air for sintered specimen and single crystal [8] of bcc $6Bi_2O_3 \cdot SiO_2$.

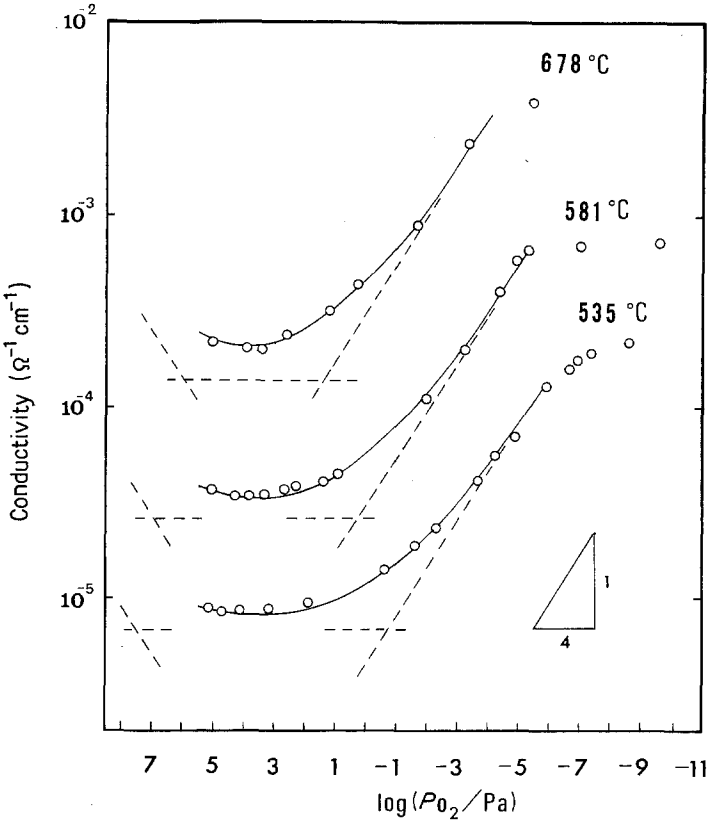

Figure 4 P_{O_2} dependence of electrical conductivity for sintered bcc $6Bi_2O_3 \cdot SiO_2$. --- separate ion, hole and electron conductivity; —— sum of the conductivity.

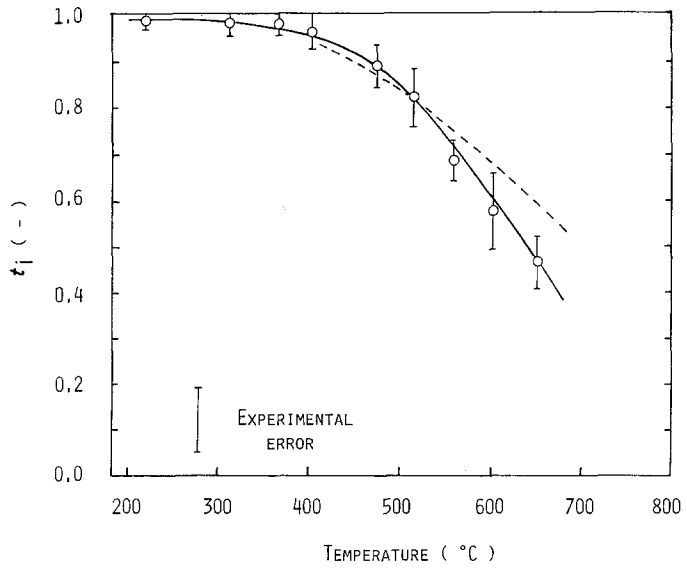

Figure 5 Temperature dependence of ionic transference number at P_{O_2} of $10^{4.33}$ (air) to $10^{3.3}$ Pa. Dashed line is calculated value from Equations 7 to 9.

trode to give an activity ratio across the specimen of 1/10 (30 to 43 mV) so that the measured transference numbers correspond to the average value for P_{O_2} between $10^{4.33}$ (air) and about $10^{3.3}$ Pa. The transference number decreased with increasing temperature, which is a similar tendency to that expected from the P_{O_2} dependences of the conductivity in the high P_{O_2} region. After the polarization measurements, morphological changes in the specimens were not found; those would be expected if charge transport by cations occurred.

The P_{O_2} dependence of the Seebeck coefficient at 700° C is shown in Fig. 6. The sign of the Seebeck coefficient changes from plus to minus at 10^3 Pa, which is very close to the P_{O_2} at the minimum of the conductivity shown in Fig. 4. Therefore, this result proves the change of the major charge carrier from the positive hole or oxygen vacancy to the electron with decreasing P_{O_2}.

Composition analysis in the sintered specimens showed that the bismuth concentration was almost equal to the theoretical value, whereas the silicon concentration was slightly less than the theoretical value. The atomic ratio Si/Bi (theoretical value 1/12) was $0.95 \pm 0.02/12$ from atomic absorption spectroscopy and $0.93 \pm 0.01/12$ from spectrophotometry. These deviations are assumed to be caused by adsorbed water in the starting SiO_2 powder or to imperfect reaction of SiO_2 with Bi_2O_3. When SiO_2 is left unreacted in the specimens it cannot be detected due to its insolubility in acid water. Probably, the partial polymorphic transformation above 680° C shown in Figs. 2 and 3 would arise from this deviation in composition.

Generally, holes and electrons in oxygen ion conductors are generated by the following defect equilibriums;

$$1/2\ O_2 + V_{\ddot{O}} = O_0^* + 2h^{\cdot} \quad (2)$$

$$O_0^* = 1/2\ O_2 + V_{\ddot{O}} + 2e' \quad (3)$$

where O_0^* is an oxygen atom at a normal oxygen site, $V_{\ddot{O}}$ is a doubly ionized oxygen vacancy and $h^{\cdot}$ and e' are a hole and an electron, respectively. When the concentration of oxygen vacancy is fixed by a charge compensation for introduced impurities or a deviation in cationic composition, such as $2[V_{\ddot{O}}] = 4[V_{Si}''''']$ for a neutrality condition, the mass action law gives the P_{O_2} dependences of $P_{O_2}^{1/4}$ and $P_{O_2}^{-1/4}$ for hole and electron conductivity, respectively [14]. Even if holes are generated according to the following equilibrium:

$$1/2\ O_2 = O_i'' + 2h^{\cdot} \quad (4)$$

where O_i'' is an interstitial oxygen ion, hole conductivity would show the $P_{O_2}^{1/4}$ dependence in the presence of oxygen vacancies with a fixed concentration [15], since an equilibrium between interstitial oxygen ions and oxygen vacancies must also be satisfied such that

$$O_0^* = V_{\ddot{O}} + O_i'' \quad (5)$$

The electron conductivity in the bcc $6Bi_2O_3 \cdot SiO_2$ was proportional to $P_{O_2}^{-1/4}$ as shown in Fig. 4. This indicates the ionic conductivity independent

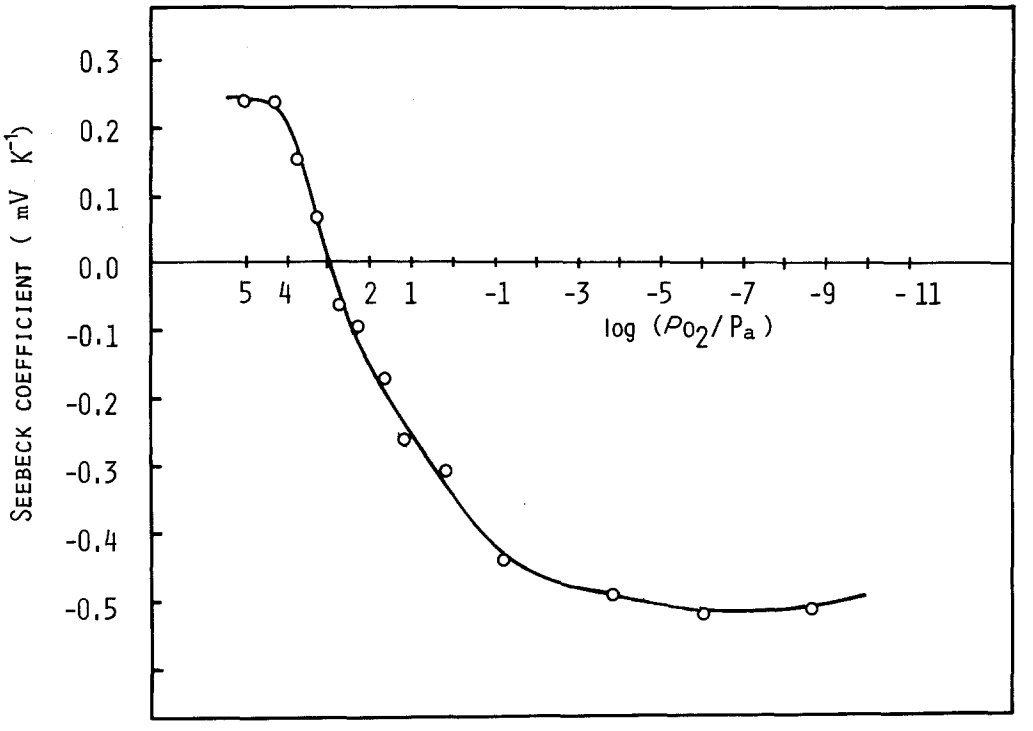

Figure 6 P_{O_2} dependence of Seebeck coefficient at 700° C for bcc $6Bi_2O_3 \cdot SiO_2$.

of P_{O_2} and the hole conductivity proportional to $P_{O_2}^{1/4}$, and hence total conductivity σ_t can be expressed as;

$$\sigma_t = \sigma_i + \sigma_p^0 \cdot (P_{O_2}/10^5\ \text{Pa})^{1/4} + \sigma_n^0 \cdot (P_{O_2}/10^5\ \text{Pa})^{-1/4} \quad (6)$$

where σ_i is the oxygen ion conductivity and σ_p^0 and σ_n^0 are the hole and electron conductivity at a P_{O_2} of 10^5 Pa, respectively. The oxygen ion, hole and electron conductivity at a P_{O_2} of 10^5 Pa, which are separated from the total conductivity so as to satisfy the Equation 6, are shown in Fig. 7. Each conductivity can be expressed as;

$$\sigma_i\ (\Omega^{-1}\ \text{cm}^{-1}) = 4.04 \times 10^3 \exp\left[-135\ (\text{kJ mol}^{-1})/RT\right] \quad (7)$$

$$\sigma_p^0\ (\Omega^{-1}\ \text{cm}^{-1}) = 1.50 \times 10^6 \exp\left[-185\ (\text{kJ mol}^{-1})/RT\right] \quad (8)$$

$$\sigma_n^0\ (\Omega^{-1}\ \text{cm}^{-1}) = 6.73 \times 10^5 \exp\left[-195\ (\text{kJ mol}^{-1})/RT\right] \quad (9)$$

where R and T have their ordinary meanings. The ionic transference numbers calculated using the Equations 7 to 9 at a P_{O_2} of 10^5 Pa are also shown in Fig. 5. The measured transference numbers are in good agreement with the calculated numbers although the measured values are somewhat smaller. The polarization method used in the present study assumes that leakage currents and electrode-gas conductance are negligibly small [16]. Actually, those effects cannot be eliminated perfectly and hence these may cause the lower value of the measured transference numbers.

The conductivity of the bcc $6Bi_2O_3 \cdot SiO_2$ single crystal measured in air presented by Kilner *et al.* [8] is shown in Fig. 7. It has values and an activation energy close to the hole conductivity of the sintered specimens. Kilner *et al.* also determined the diffusion coefficient of oxygen using the ^{18}O tracer diffusion profile in the single crystal. An estimated oxygen ion conductivity from the diffusion coefficient was approximately 3×10^{-10} (Ω^{-1} cm^{-1}) at 500° C, which is much lower than that in the present study.

Since Bi^{3+} ions (0.111 nm) are too large to be situated at tetrahedrally coordinated Si^{4+} (0.026 nm) sites [17], it is expected from the deviation in cation atomic ratio that silicon vacancies are present in the sintered specimen. Craig and Stephenson [18] have performed X ray analysis on the bcc compounds of ZnO–Bi_2O_3 or Fe_2O_3–Bi_2O_3 systems and suggested that pentavalent

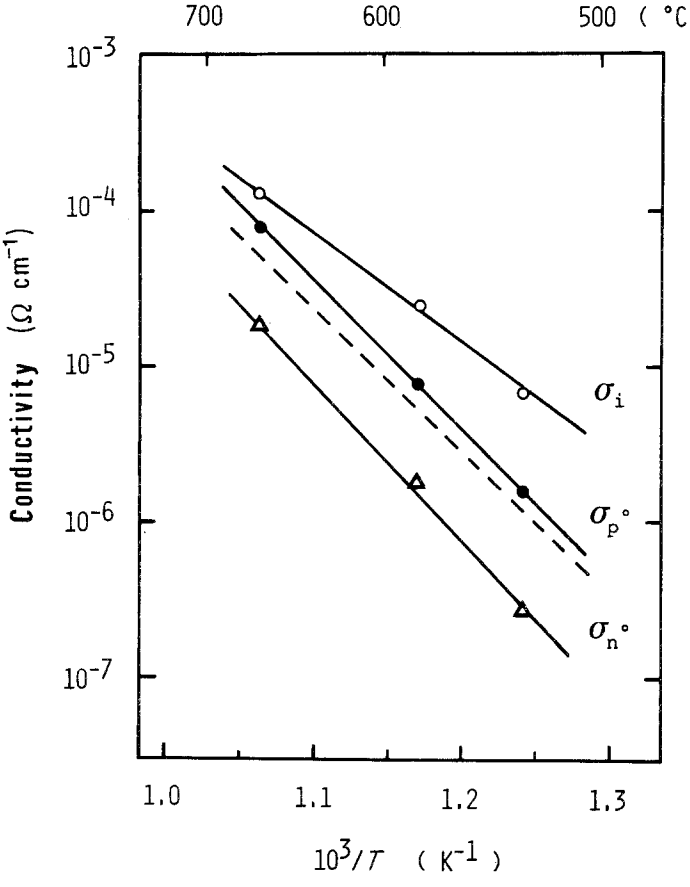

Figure 7 Temperature dependences of oxygen ion (σ_i), hole (σ_p^0) and electron (σ_n^0) conductivity at P_{O_2} of 10^5 Pa in sintered bcc $6Bi_2O_3 \cdot SiO_2$. Dashed line shows electronic conductivity in single crystal in air [8].

bismuth ions substitute on the tetrahedral sites leaving the electron population constant on each tetrahedral site. However, it is difficult to explain the much increased oxygen ion conductivity either by the substitution of Bi^{5+} ions at tetrahedral sites or by oxygen diffusion through grain boundaries. Furthermore, if the anion sub-lattice is occupied perfectly, silicon vacancies would dissociate and generate holes, resulting in an increase of hole conductivity. Therefore, Schottky-type defects may be present in the nonstoichiometric specimens and the increased oxygen ion conductivity would be attributed to the silicon and oxygen ion vacancies. Probably the dominant neutrality condition for the defect equilibriums is $2[V_{\ddot{O}}] = 4[V_{Si}''']$, as expected from the P_{O_2} dependences of conductivity. The existence of silicon and oxygen ion vacancies is proposed also in the single crystals on the basis of optical measurements [19].

Oxygen partial pressures $P\oplus$ and $P\ominus$, at which the hole and electron conductivity are equal to the oxygen ion conductivity, respectively, can be obtained from the P_{O_2} dependences of conductivity. They are expressed as a function of absolute temperature as;

$$\log (P\oplus/\text{Pa}) = (8.50 \times 10^3/T) - 3.04 \quad (10)$$

$$\log (P\ominus/\text{Pa}) = (-10.8 \times 10^3/T) + 12.81 \quad (11)$$

and shown in Fig. 8. Fig. 8 is also a semiquantitative diagram of dominant conduction mechanisms in the nonstoichiometric bcc $6Bi_2O_3 \cdot SiO_2$ in the present study.

5. Conclusions

The P_{O_2} dependence of electrical conductivity and Seebeck coefficient and the temperature dependence of ionic transference number showed that sintered bcc $6Bi_2O_3 \cdot SiO_2$ was a mixed conductor, in which electron conductivity was proportional to $P_{O_2}^{-1/4}$ and predominant below 10^{-1} Pa.

The activation energy at a P_{O_2} of 10^5 Pa was found to be 135, 185 and 191 kJ mol^{-1} for oxygen ion, hole and electron conduction, respectively, at 535 to 678° C.

Silicon concentration in the specimen was

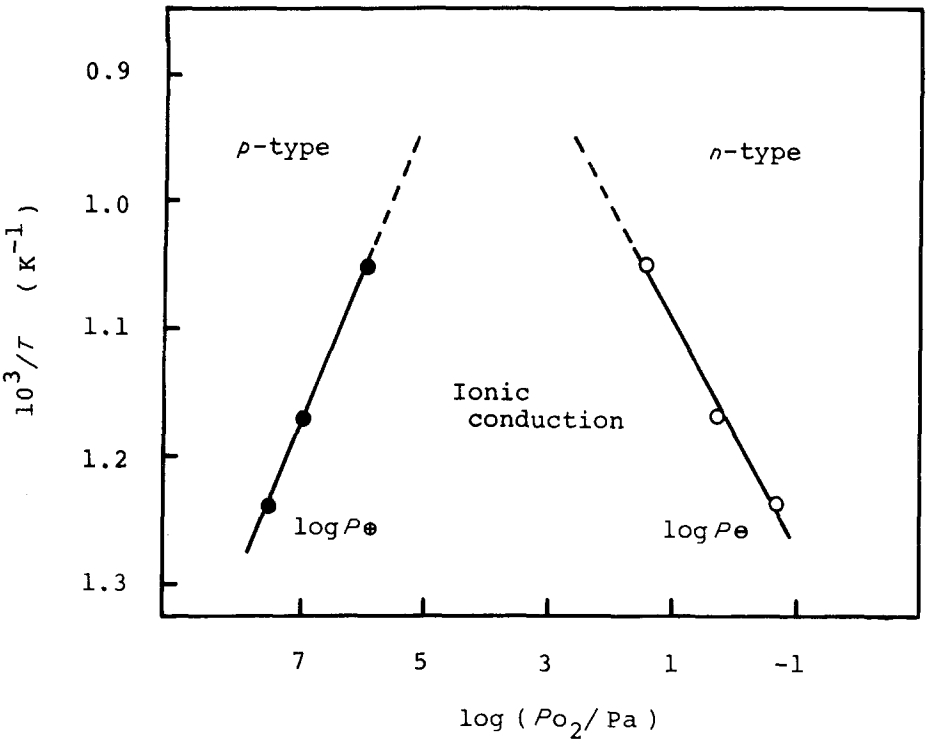

Figure 8 log $P_\oplus$ and log $P_\ominus$ against $1/T$ for sintered bcc $6Bi_2O_3 \cdot SiO_2$.

slightly less than the theoretical value, resulting in cation atomic ratio Si/Bi of 0.93 to 0.95/12 (theoretically 1/12). Schottky-type defects of silicon and oxygen vacancies were proposed to explain a much higher oxygen ion conductivity in the sintered specimen when compared with the reported value in single crystals.

Acknowledgement

The authors wish to thank Mr Y. Shimizu for analysis of cationic composition.

References

1. L. G. SILLEN, *Ark. Kemi. Mineral. Geol.* 12A (1937) 1.
2. E. M. LEVIN and R. S. ROTH, *J. Res. Nat. Bur. Stand. Sect. A* 68 (1964) 197.
3. S. C. ABRAHAMS, P. B. JAMIESON and J. L. BERNSTEIN, *J. Chem. Phys.* 47 (1967) 4034.
4. H. A. HARWIG, *Z. Anorg. Allg. Chem.* 444 (1978) 151.
5. R. E; ALDRICH, S. L. HOU and M. L. HARVILL, *J. Appl. Phys.* 42 (1971) 493.
6. S. L. HOU, R. B. LAUER and R. E. ALDRICH, *J. Appl. Phys.* 44 (1973) 2652.
7. H. SCHWEPPE and P. QUADFLIEG, *IEEE Trans. Sonics Ultrasonics* SU-21 (1974) 56.
8. J. A. KILNER, J. DRENNAN, P. DENNIS and B. C. H. STEELE, *Solid State Ionics* 5 (1981) 527.
9. T. TAKAHASHI, H. IWAHARA and T. ESAKA, *J. Electrochem. Soc.* 124 (1977) 1563.
10. M. J. VERKERK and A. J. BURGGRAAF, *ibid.* 128 (1981) 75.
11. HO-KUN KIM, T. KOKUBO, S. ITO and M. TASHIRO, *Yogyo Kyokai Shi* 90 (1982) 348.
12. M. MIYAYAMA, S. KATSUTA and H. YANAGIDA, *Nihon Kagakukai Shi* 1981 (1981) 1583.
13. O. H. HILL and J. C. BRICE, *J. Mater. Sci.* 9 (1974) 1252.
14. R. J. BROOK, in "Electrical Conductivity in Ceramics and Glass" Part A, edited by N. M. Tallan (Marcel Dekker, New York, 1974) p. 179.
15. M. F. LASKER and R. A. RAPP, *Z. Physik. Chem. Neue Folge* B49 (1966) 198.
16. R. W. VEST and N. M. TALLAN, *J. Appl. Phys.* 36 (1965) 543.
17. R. D. SHANNON and C. T. PREWITT, *Acta Crystallogr.* B25 (1969) 925.
18. D. C. CRAIG and N. C. STEPHENSON, *J. Solid State Chem.* 15 (1975) 1.
19. M. PELTIER and F. MICHERON, *J. Appl. Phys.* 48 (1977) 3683.

Received 13 December 1982
and accepted 18 February 1983